New Pilot Protection Method Based on the Current Fault Component Waveform Similarity

Shuping Gao[1], Han Zheng[1], Yue Gao[2], and Guobing Song[3]

[1]Xi'an Scientific and Technological University
[2]Xi'an University of Science and Technology
[3]Xi'an Jiaotong University

May 12, 2023

Abstract

In order to improve the ability of the modular multi-level converter to quickly clear and isolate faults in the multi-terminal flexible DC grid, this paper analyzes the characteristics of current faults in the multi-terminal flexible direct current grid, introduces the comprehensive distance of current fault waveform, and proposes a line protection method based on the similarity of current fault waveform. This protection method firstly uses Euclid DTW (Dynamic Time Warping) distance and entropy weight method to process electrical quantity signals, calculates the comprehensive distance of current fault waveform of two converter stations, and builds the protection criterion based on the similarity of current fault waveform. Then, the fault identification is realized by using the calculated comprehensive distance, and the fault pole identification is realized by using the ratio of comprehensive distance between positive and negative poles. Finally, PSCAD was used to build a simulation model to output the fault data under different fault conditions, and MATLAB was used to process the fault data to verify the protection algorithm. The simulation results show that the proposed method has good resistance to high resistance, and its rapidity and adaptability are further improved. The research results will provide a theoretical basis for the safe and reliable operation of flexible DC power grid.

New Pilot Protection Method Based on the Current Fault Component Waveform

Similarity

Shuping Gao[1,2], Han Zheng [1,2*], Yue Gao [1,2], Guobing Song [3]

[1] School of Electrical and Control(Xi 'an University of Science and Technology), Xi 'an, China

[2] Xi'an Key Laboratory of Electrical Equipment Condition Monitoring and Power Supply Security Xi'an 710054,China

[3] School of Electric Engineering(Xi'an Jiaotong University), Xi'an, China

[*] *1535755497@qq.com*

Abstract—**In order to improve the ability of the modular multi-level converter to quickly clear and isolate faults in the multi-terminal flexible DC grid, this paper analyzes the characteristics of current faults in the multi-terminal flexible direct current grid, introduces the comprehensive distance of current fault waveform, and proposes a line protection method based on the similarity of current fault waveform. This protection method firstly uses Euclid DTW (Dynamic Time Warping) distance and entropy weight method to process electrical quantity signals, calculates the comprehensive distance of current fault waveform of two converter stations, and builds the protection criterion based on the similarity of current fault waveform.**

Then, the fault identification is realized by using the calculated comprehensive distance, and the fault pole identification is realized by using the ratio of comprehensive distance between positive and negative poles. Finally, PSCAD was used to build a simulation model to output the fault data under different fault conditions, and MATLAB was used to process the fault data to verify the protection algorithm. The simulation results show that the proposed method has good resistance to high resistance, and its rapidity and adaptability are further improved. The research results will provide a theoretical basis for the safe and reliable operation of flexible DC power grid.

Index Terms—**Euclidean distance, entropy weight method, flexible direct current power grid, pilot protection, waveform similarity.**

Introduction

To integrate and accommodate large-scale renewable generations such as wind power and solar power, multi-terminal flexible DC grid (MTFDC) based on modular multi-level converter (MMC)-HVDC has been widely used as a promised solution due to its independent power regulation and flexible operation capabilities, small switching loss and strong expansibility [1-5]. However, the stable and reliable operation of MTFDC is heavily dependent upon the fast and reliable DC line protection [6]. The protection scheme of the DC line can be categorized as two types: single-ended quantity protection and double-ended quantity protection according to the extracted electrical quantity of converter station from one-end or both-end of the DC line [7-23].

Typical single-ended quantity protection schemes on the MTFDC grid mainly include boundary protection, transient voltage protection and voltage traveling wave protection [7-13], and so on. In [7-8], the protection principles proposed are based on the change rate of voltage measured at the line side of DC inductors. However, the reliability under high-resistance faults cannot be guaranteed and the required sampling frequency is much high. In [9], a protection method using the change rate of the DC inductor voltage is proposed. In [10], a single-ended transient-voltage-based protection strategy for a flexible DC grid was proposed. The proposed method has higher reliability and stronger ability to endure high transition resistance, but the high transition resistance is only 300Ω. In [11], the method based on the high-frequency components of transient voltages on DC lines is proposed, which has fast operation speed and good robustness. However, an accurate theoretical basis is not analyzed thoroughly. In [12], according to the second-order difference of backward voltage traveling wave, a protection scheme is proposed. The high-resistance problem is overcome, but the required time window is more than 3ms. In [13], the method based on transient high-frequency energy of line current is proposed. Lumped parameter-based DC line model cannot reflect the propagation process of traveling waves on long transmission lines. According to the above analysis, the single-end protection can identify internal fault and external fault quickly without communication only by using the one-end data of the DC line, but it also has some disadvantages such as weak resistance to high transition resistance and low sensitivity.

As for double-ending protection, many achievements mainly focus on traveling waves, line boundary elements, transient impedance[14-25], etc. In [14], a protection scheme is proposed, which is based on the time difference between the initial forward and backward traveling waves reaching the relays on both ends of the DC line. In [15-16], the protection methods can be implemented by the voltages of DC inductors on both ends of the DC line. In [17], the protection principles are both based on the ratio of the transient voltages (ROTV) at both sides of the DC inductor. To ensure the reliability under high-resistance faults, the ROTVs at both ends of the DC line are required. In [18], a protection method based on the transient measured impedance is proposed. In [19], short-time energy is used to identify DC single-pole ground fault in a multi-terminal flexible DC system. In [20-21], the ratio of electrical fault quantity at both ends of the line is selected to identify internal and external faults. In [21], protection based on incremental reactive power coefficients (IRPCs) is proposed. The protection principles can be carried out by the both-end data of the DC line, which can meet the absolute selectivity of fault identification. However, due to the communication delay, some algorithms require strict synchronization of double-terminal data and high error measurement ability, which limits the rapidity of protection. Besides, a large short-circuit current will be generated in an ultrashort time after DC fault occurs in multi-terminal power transmission systems, which can damage the semiconductor devices and even lead to the blocking of the converter station if the fault cannot be cleared quickly[22]. In [24], a new protection scheme for flexible distribution system based on cosine similarity of DC current waveform is proposed. The proposed protection scheme can identify internal faults in less than 0.3 millisecond with good reliability and high sensitivity. And it is robust to distributed capacitance, and not requires strict communication synchronization. In [25], an adaptive reclosing scheme based on the transient current waveform similarity matching is proposed. The protective reach of reclosing criterion proposed can cover the entire transmission line, with high sensitivity and well applicability.

In [26], a new scheme of traveling wave longitudinal protection based on measuring wave impedance Euclidean distance is put forward, the protection principle can identify internal and external faults with reliably, sensitively and quickly, and has a strong ability to withstand transition resistance and noise interference. In [27], load curve clustering method based on Euclidean Dynamic Time Warping Distance and Entropy Weight is introduced, which can be used in power system protection principle.

In view of the above reasons, in order to improve the ability of the modular multi-level converter to quickly clear and isolate faults in the multi-terminal flexible direct current grid, it is necessary to study a new type of protection methods for DC grid.

This paper analyzes the characteristics of current faults in the multi-terminal flexible direct current grid, introduces the comprehensive distance of current fault waveform, and proposes a line protection method based on the similarity of current fault waveform. The proposed method has good resistance to high resistance, and its rapidity and adaptability are further improved.

The remainder of this paper is organized as follows. In Section 2, the topology of the four-terminal MMC flexible DC grid is introduced; In Section 3, the current fault characteristics are analyzed; In Section 4, the measurement methods of the current fault component waveform similarity are introduced; In Section 5, the protection criteria and protection principal flow chart of are introduced; In Section 6, simulation verifications are carried out in MATLAB; And conclusions are given in Section 7.

Topological Structure of Modular Multi-terminal Flexible DC Grid with Multi-level Converter

This paper analyzes the characteristics of Zhangbei four-terminal ring flexible DC power grid. The system is a four-terminal symmetrical bipolar MMC flexible DC transmission line with a DC voltage level of ±500kV, and the length of each line is marked according to the actual length. Topology and fault location are shown in Fig.1. A series of small inductors are added to the DC side of each station to construct the boundary conditions. According to the actual situation, the parameter is 0.3H.

Hosted file

`image1.emf` available at https://authorea.com/users/617453/articles/642877-new-pilot-protection-method-based-on-the-current-fault-component-waveform-similarity

P1~P8—positive pole on both sides of the converter station protection measurement installation point; N1~N8—negative pole on both sides of the converter station protection measurement installation point; f1—positive pole grounding fault; f2—Negative grounding fault; f3—Bipolar transversal fault; f4—Bipolar short circuit grounding fault; f5~f8—Exterior fault of DC line exit of converter station.

Fig.1 Topology of the four-terminal MMC flexible DC grid

Analysis of Waveform Characteristics of Current Fault

3.1 Fault interval identification of multi-terminal DC grid

When the system is in normal operation, the current waveform changes regularly, and the load current is traversing current. It is defined that the positive direction of the current is from the converter station bus to the DC line. Because the current on the DC side has only polarity and no phase, the current waveform of the converter station at both ends has no change and the polarity is positively correlated.

Combined with the four-terminal MMC flexible direct current grid topology, it is still assumed that a positive ground fault (f_1) occurs between B3 and F1 stations, and the difference of current fault waveforms between fault lines (L3) and non-fault lines (L2 and L4) is analyzed. In the dashed line interval shown in Fig.1, the equivalent diagram of the fault line is shown in Fig.2.

Hosted file

`image2.emf` available at https://authorea.com/users/617453/articles/642877-new-pilot-protection-method-based-on-the-current-fault-component-waveform-similarity

Fig .2 A fault line equivalent diagram when a fault at f1 position between B3 and F1 occurs

As can be seen from Fig.2, when a fault of f_1 position occurs between the B3 station and the F1 station, the current waveform and polarity of the six protection measurement installation points will change, and the current of each measurement point will flow to the fault point. Therefore, the positive and negative correlation of the current measured at each line protection measurement installation point will change accordingly. The current fault component waveforms extracted from the two protection measurement installation points (4 and 5) on the fault line have a large change and they are positive correlation, and the distance between the two current fault component waveform is smaller than the preset setting value. While the current fault component waveforms extracted from the non-fault interval protection measurement installation point (2,3 or 6,7) have a small change and they negative correlation, and the distance between the two current fault component waveform (2,3 or 6,7) is larger than the preset setting value. Therefore, based on the difference of fault characteristics, it is determined whether the fault occurs between the B3 and the F1 station, that is, on the line L3. If the fault occurs on the line, the corresponding protection element is activated.

3.2 Internal and External Fault Characteristic Analyses

The physical boundary of a DC line is defined as the flat wave reactor on that line and the fault is classified as internal or external fault. After determining the interval of the converter station where the fault occurred, it is further determined whether the fault occurred on the DC transmission line, i.e., the internal and external fault characteristics are carried out. The type of fault is determined by the setting values and comparing them with the collected current signals.

Therefore, combined with the superposition theorem, the fault additional network can be obtained as shown in Fig. 3 and 4. UP4 and UN4 are the positive and negative transient voltage components at the 4th protection measurement installations respectively, UP5 and UN5 are the positive and negative transient voltage components at the 5th protection measurement installations respectively. iP4 and iN4 are the positive and negative fault currents at the 4th protection measurement installations respectively, iP5 and iN5 are the positive and negative fault currents at the 5th protection measurement installations respectively. ZP4X, ZP5X, ZN4X and ZN5X are the positive and negative equivalent impedances on the AC side of the two converter stations, ZP4 and ZP5 are the equivalent impedances at fault points 4 and 5 respectively, and Zh is the non-fault line equivalent impedance.

3.2.1 Internal fault characteristics analyses : When a fault occurs in the DC line, the additional network for each fault is shown in Fig.3. i_{f1} -i_{f4} are the actual fault currents in the line area after the occurrence of the fault, respectively, and the current flows in the direction shown by the arrows in Fig.3.

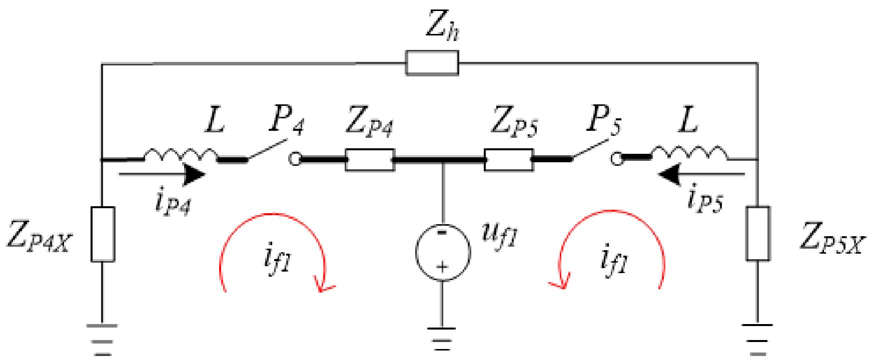

(a)Additional network diagram at the fault point$f$ $_1$

(b) Additional network diagram at the fault pointf_2

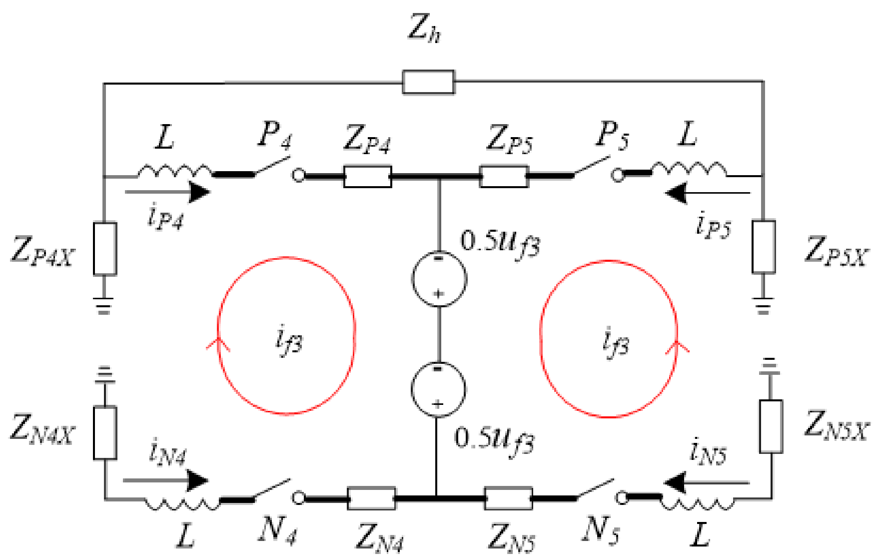

(c) Additional network diagram at the fault point$f$ $_3$

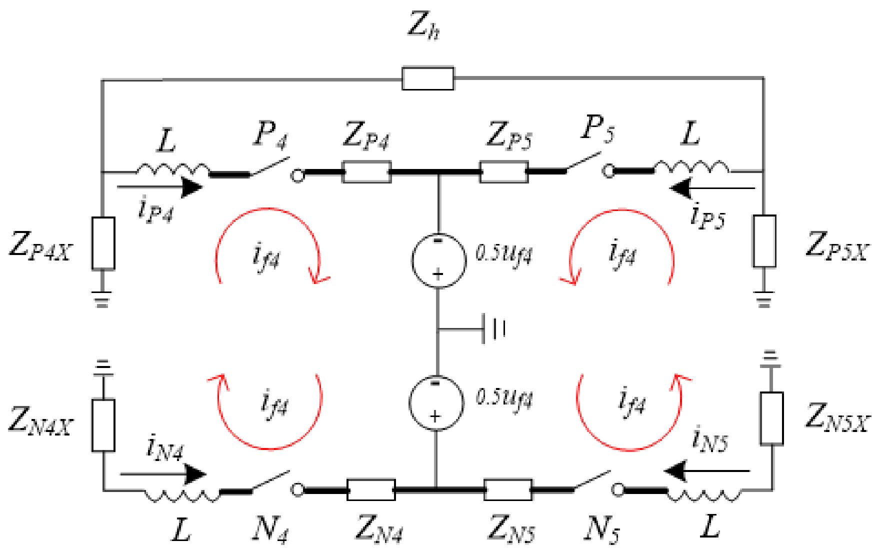

(d) Additional network diagram at the fault pointf_4

Fig.3 Additional network diagram when an internal fault occurs

From Fig.3 (a) can be seen, when a positive ground fault (f_1) occurs in the DC line, the line currents at both ends flow from the converter station to the fault point. Protection installation at 4 and 5 positive pole waveform polarity taken is positive, the waveform is positively correlated, the fault waveform distance is small, less than the setting value.

From Fig.3(b) can be seen, when a negative ground fault (f_2) occurs in the DC line, the line currents at both ends flow from the fault point to the converter station. Protection installation 4 and 5 negative pole waveform polarity taken is negative, waveform is positively correlated, the fault waveform distance is small, less than the setting value.

From Fig.3 (c) and (d) can be seen, when a double pole across the fault (f_3) or double pole ground fault (f_4) occurs in the DC line, the currents at both ends of positive line flow from the converter to the fault point, the polarity of the waveform taken is positive; the currents at both ends of negative line are flowing from the fault point to the converter, the polarity of the waveform taken is negative. Positive and negative waveforms are positively correlated, and the current fault waveform distance is smaller than the setting value.

Therefore, from the above analysis can be obtained that when an internal fault occurs, the fault pole current waveform at protection installation 4 and 5 will change, the current fault waveform of both sides is positively correlated and the similarity is high. 4 and 5 fault current polarity and similarity are shown in Table 1.

Table 1 Polarity and correlation of the current fault component at the protection installations of 4 and 5 when an internal fault occurs

Type of fault	I_{P4}	I_{P5}	I_{N4}	I_{N5}	Similarity
f_1	+	+	-	-	Positive
f_2	+	+	-	-	Positive
f_3	+	+	-	-	Positive
f_4	+	+	-	-	Positive

3.2.2 External fault characteristics analyses: When an external fault occurs outside the DC line, the additional network for each fault is shown in Figure 4. i_{f5} -$i_{f8}$are the actual fault currents after the occurrence of an external fault, respectively, and the current flows in the direction shown by the arrows in Fig.4.

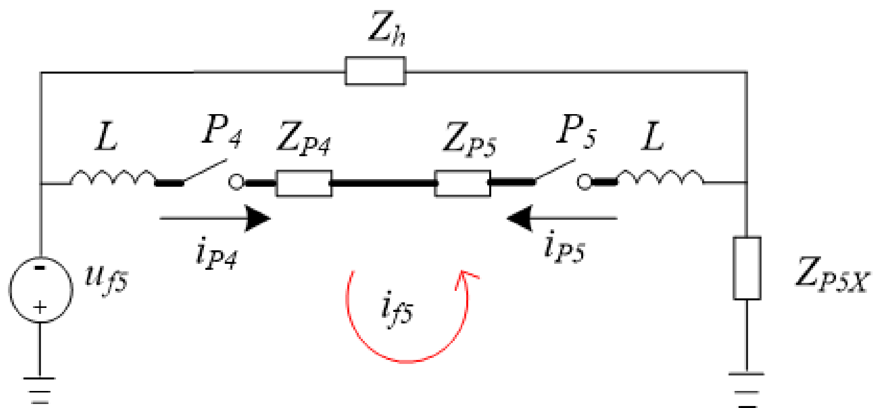

(a)Additional network diagram at the fault point f_5

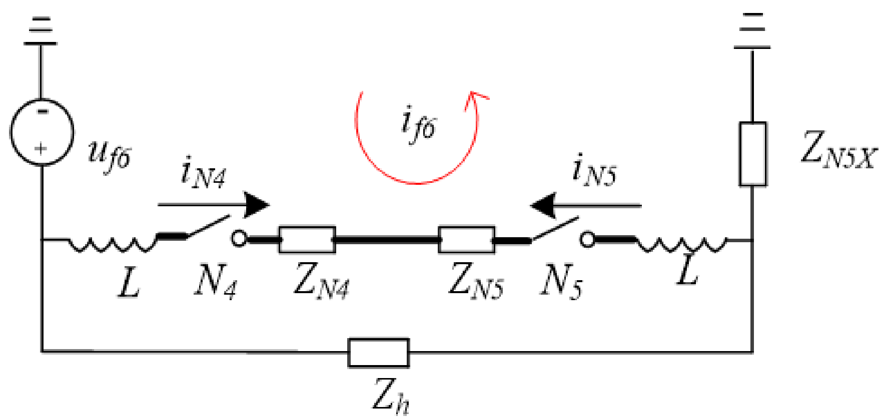

(b) Additional network diagram at the fault point f_6

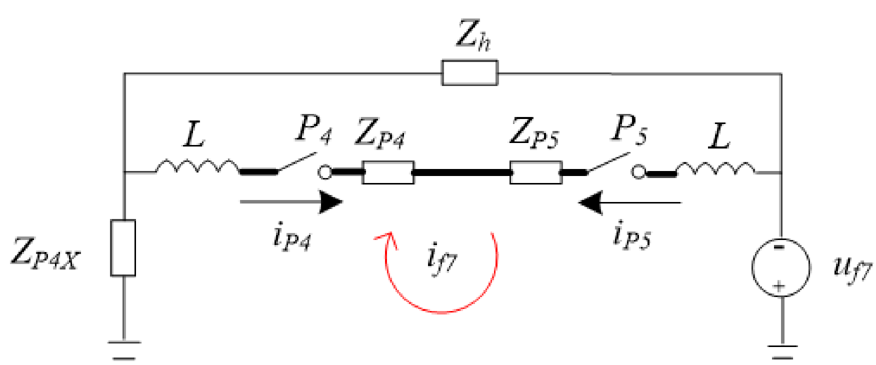

(c) Additional network diagram at the fault point f_7

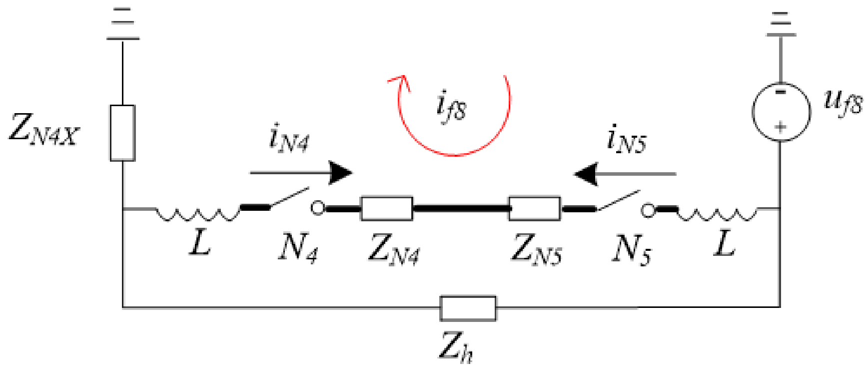

(d) Additional network diagram at the fault point f_8

Fig.4 Additional network diagram when an external fault occurs

As can be seen in Fig.4, when an external fault occurs beyond the line, protection devices are installed at 4 and 5 positions. The fault currents are flowing from the converter station to the fault point. However, for different types of faults, the polarity of the fault current waveform taken by the converter station on both sides will then change.

From Fig. 4 (a) and 4 (d), it can be seen that when the fault occurs atf_5 or f_8 point, the polarity of the positive and negative fault current waveforms at 4 locations is negative, and the polarity of the positive and negative fault current waveforms at 5 locations is positive. From Fig. 4 (b) and 4 (c), it can be seen that when the fault occurs atf_6 or f_7 point, the polarity of the positive and negative fault current waveforms at 4 location is positive, and the polarity of the positive and negative fault current waveforms at 5 locations is negative.

Therefore, from the above analysis it can be obtained that when an external fault occurs, two current fault waveforms taken at the protection device of 4 and 5 positions are negatively correlated, the fault waveform distance is larger than the setting value, similarity is low. 4 and 5 fault current polarity and similarity are shown in Table 2.

Table 2 Polarity and correlation of the current FAULT component at the protection installations of 4 and 5 when an external fault occurs

Type of fault	IP4	IP5	IN4	IN5	Similarity
f5	-	+	-	+	Negative
f6	+	-	+	-	Negative
f7	+	-	+	-	Negative
f8	-	+	-	+	Negative

3.3 Fault Pole Selection

After a fault has occurred, the sound pole will be affected by the fault pole due to the presence of line coupling and a certain fault current component will be induced. Therefore, it is essential that fault pole selection is carried out by selecting a suitable setting value.

When a positive fault occurs on the DC line, the distance between the positive fault waveforms at 4 and 5 is smaller and the negative fault waveforms are larger, so the ratio of the positive and negative fault waveforms is smaller and smaller than the setting value; when a negative fault occurs on the DC line, the distance between the positive fault waveforms at 4 and 5 is larger and the negative fault waveforms are smaller, so the ratio of the positive and negative fault waveforms is larger and larger than the setting value; when a bipolar fault occurs, the difference between the positive and negative fault waveforms is smaller and the ratio of the positive and negative fault waveforms is around the setting value. When a bipolar fault occurs, the difference between the positive and negative fault waveforms is smaller, and the ratio of the positive and negative fault waveforms is around the setting value. Therefore, the ratio of the positive and negative fault waveform distances is used to construct a pole selection criterion, which can be used to identify fault and sound poles.

Measurement of current fault component waveform similarity

Considering the following three characteristics of the current fault component, the similarity of its waveform is measured comprehensively:

The overall distribution characteristic, i.e., the overall similarity of the fault waveform is reflected by the magnitude of the distance of the sampling points at the same time of the curve;

(2) Overall dynamic characteristics, i.e., similarity is measured by comparing the corresponding fault waveforms in the sampling time period;

(3) Local dynamic characteristics, i.e., similarity is measured by comparing the average rate of change of the fault waveform at the same sampling interval.

4.1 Euclidean Distance

The Euclidean distance is used to measure the true distance between two points in m-dimensional space. It can reflect the overall distribution characteristics of waveform similarity.

The fault current components at protection installation points 4 and 5 are extracted and defined as XP4, XN4, XP5 and XN5 respectively, where XP4 = (x1, x2, . . . , xn), XN4 = (y1, y2, . . . , yn), XP5 = (z1, z2, . . . , zn), XN5 = (q1, q2, . . . , qn). Then the Euclidean distance of the waveform at the protection installation points on both sides can be obtained as equations (1) and (2).

$$D_{\mathrm{WP}}\left(X_{P4}, X_{P5}\right)=\sqrt{\sum_{i=1}^{n}\left(x_i-z_i\right)^2} \tag{1}$$

$$D_{\mathrm{WN}}\left(X_{N4}, X_{N5}\right)=\sqrt{\sum_{i=1}^{n}\left(y_i-q_i\right)^2} \tag{2}$$

Where DWP and DWN represent the waveform Euclidean distance between the positive and negative poles of the protection device points on both sides respectively. n represents the number of sampling points, which can be selected according to actual accuracy requirements.

4.2 DTW distance

Unlike Euclidean distance, DTW (Dynamic Time Warping) does not carry out distance calculation strictly according to the corresponding value of the same sampling point of the sequence. It adopts the idea of dynamic programming to adjust different sampling points of sampling sequence, explore the relationship between corresponding elements, and optimize the curved path.

The algorithm can well describe the overall dynamic characteristics of curves and measure the overall shape similarity between sequences. It is suitable for the situation where the fault waveforms of two converter stations have good overall similarity, but they are not completely aligned at the sampling points.

For the sampling sequence XP4 and XP5, the n $\times$ m distance matrix DP is constructed, where the elements are DP (i, j) in equation (3); for XN4 and XN5 the distance matrix DN is constructed, where the elements DN (i, j) in equation (4). Equation (3) represents the Euclidean distance between the sampling sequence

XP4 and the XP5 sequence points xi and zj , and Equation (4) represents the Euclidean distance between the sampling sequence XN4 and the XN5 sequence points yi and qj.

$$D_P\left(i,j\right)=\sqrt{\left(x_i-z_j\right)^2}\qquad 1\leq i\leq n,1\leq j\leq m \tag{3}$$

$$D_N\left(i,j\right)=\sqrt{\left(y_i-q_j\right)^2}\qquad 1\leq i\leq n,1\leq j\leq m \tag{4}$$

The data set consisting of each group of adjacent elements in DP (i, j) and DN (i, j) is called the curved path of the collected waveform and is denoted as L = {l1 , l2 , [?]ls , [?], lk } and R = {r1 , r2 , [?]rs , [?], rk }. Where the element ls is the coordinate of the sth point on the path L, i.e., ls = (i, j), and the element rs is the coordinate of the sth point on the path R, i.e., rs = (i, j). At the same time, the paths L and R should satisfy the following two-part constraints. One is that the selected paths need to contain all sampling points, i.e., l1 = (1, 1) and ls = (n, m), the other is that each sampling point needs to match with the adjacent sampling points, i.e., if ls = (i, j), then ls+1 = (a, b) satisfies 0 [?] a - i [?] 1 and 0 [?] b - j [?] 1. Therefore, the DTW distance between the sampling sequences XP4 and XP5 is defined by equation (5), and the DTW distance between the sampling sequence XN4 and XN5 is defined as equation (6).

$$D_{\text{Pdtw}}\left(X_{P4},X_{P5}\right)=\sum_{s=1}^{k}D\left(L_s\right) \tag{5}$$

$$D_{\text{Ndtw}}\left(X_{N4},X_{N5}\right)=\sum_{s=1}^{k}D\left(R_s\right) \tag{6}$$

Where D(Ls) and D(Rs) are the cumulative distances of the curved paths L and R. DPdtw and DNdtw represent the waveform DTW distances between the positive and negative poles of the protection installation points on each side, respectively.

4.3 Local dynamic mapping

Because the sampling sequences of XP4, XN4, XP5 and XN5 are discrete, considering the accuracy of the algorithm, it can be converted into a morphological sequence of XP4', XN4', XP5' and XN5' with n-1 length. Among them, there exists: XP4=(x1',x2',...xn'),XN4=(y1',y2',...yn'),XP5=(z1',z2',...zn'),XN5=(q1',q2',...qn'). These morphological sequences can better describe the local dynamic characteristics of current fault component waveforms, reflect its trend information at each sampling interval. Where, the element xi' is shown in (7), yi', zi', qi' and xi' are the similar expressions.

$$x_i^{'}=\frac{x_{i+1}-x_i}{t}\qquad i=1,2,\cdots,n-1 \tag{7}$$

In (7), [?]t is the time interval.

4.4 Entropy Weight Method

Entropy weight method is an objective weight method, which uses entropy to express the characteristics of the amount of information, that is, the greater the difference between each evaluation object is, the more information it contains, the smaller its entropy is. The entropy weight method only highlights the local difference, that is, the greater the level difference between the evaluation objects is, the greater the weight of the index is and the greater the impact on the evaluation results is.

4.5 Similarity Description of Overall Current Fault Component Waveform

Based on the analysis of the fault characteristics of the current fault waveform in Section 3, combining Euclidean distance and DTW distance, a method of measuring the similarity of current fault waveforms with overall and local characteristics is proposed. Therefore, the distance of positive and negative current fault waveforms at the protection installation points on both sides are shown in equations (8) and (9).

$$D_{\text{allP}} = \alpha D_{\text{WP}}\left(X_{P4}, X_{P5}\right) + \beta D_{\text{Pdtw}}\left(X_{P4}, X_{P5}\right) + \gamma D_{\text{Pdtw}}\left(X_{P4}^{'}, X_{P5}^{'}\right) \tag{8}$$

$$D_{\text{allN}} = \alpha D_{\text{WN}}\left(X_{N4}, X_{N5}\right) + \beta D_{\text{Ndtw}}\left(X_{N4}, X_{N5}\right) + \gamma D_{\text{Ndtw}}\left(X_{N4}^{'}, X_{N5}^{'}\right) \tag{9}$$

Where DallP and DallN represent the distance between the positive and negative current fault waveforms at the protection installation point on both sides respectively. The smaller the value is, the higher the similarity between the two sides of the current fault waveform is. DWP (XP4 , XN4) and DWN (XP4 , XN4) reflect the overall distribution characteristics of the waveform respectively; DPdtw (XP4 , XN4) and DNdtw (XP4 , XN4) reflect the overall dynamic characteristics of the waveform respectively; DPdtw (XP4, , XN4,) and DNdtw (XP4, , XN4,) reflect the local dynamic characteristics of the waveform respectively. α, β and γ are the weights of each measure of distance respectively, which are taken as 0.4, 0.3 and 0.3 according to the actual sampling accuracy.

Protection Principal Implementation Process

5.1 Current Fault Waveform Extraction

When a fault occurs, the current will change and the current fault waveform will show different change features depending on the fault type. From the current fault characteristics in Section 3.1, the current fault component can be extracted by equation (10).

$$I_s\left(t\right) = I_S\left(t\right) - I_S\left(t - T\right) \tag{10}$$

Where: t is the sampling moment; Is (t) is the actual current value at t; T is the selected sampling moment before the fault occurs, generally being taken n sampling period before the fault occurs. Considering the stability of the system operation, it is taken two sampling periods before the fault occurs. ΔIs (t) is the current fault component extracted from the protection measurement installation points at t.

5.2 Protection criteria

5.2.1 Protection start criterion: When a fault occurs, the current fault component rises or falls and the protection start criterion can be constructed based on the magnitude of the current change. By extracting the change of the current fault component at each protection measurement installation, the protection start criteria are given in equation (11).

$$\begin{cases} I_P > K_{set1} = 0.1kI_n \\ I_N < K_{set2} = -0.1kI_n \end{cases} \tag{11}$$

Where: $\boldsymbol{\Delta I_{\Pi}}$ and I_N are the current fault components of the positive and negative currents respectively; K_{set} $_1$ andK_{set} $_2$ are the threshold values of the starting current of the positive and negative currents respectively;k is the reliability coefficient, generally ranging from 1.2 to 1.5; I_n is the rated current. If the start criteria are satisfied, further identification between fault and non-fault intervals is carried out.

Using equations (8) and (9) to calculate the combined distance between the positive and negative current fault waveforms at each protection measurement installation respectively, denoted as DPX and DNX, the identification criterion between the fault and non-fault intervals is determined by equation (12).

$$\begin{cases} |D_{\mathrm{PX}}| < D_{\mathrm{set1}} \\ |D_{\mathrm{NX}}| < D_{\mathrm{set1}} \end{cases} \tag{12}$$

Where: X is the variable and takes the value of each protection measurement installation point labeled as 1-8, that is P1-P8 and N1-N8 points shown in Fig.1, $|\cdot|$ indicates the modal value.

When a fault occurs in different converter station intervals, the waveform distances DPX and DNX of positive and negative current fault components in the corresponding fault intervals are smaller than the preset setting values. However, the opposite is true for the non-failure interval, the waveform distance values of them are greater than the preset setting value.

Considering the topology structure and operating conditions of DC power grid, the setting value Dset1 is taken as 0.8. When the current fault component and waveform distance between the two measurement points satisfy both equations (11) and (12), the protection of the corresponding fault interval is activated and the non-fault interval protection is blocked. According to equation (11) and equation (12), the fault interval can be reliably identified.

5.2.2 Internal and External Fault Identification Criteria: After ensuring that the non-fault line can operate correctly, further internal and external fault identifications are carried out.When the fault interval is determined, taking the flat-wave reactor as the boundary condition, the stations can be classified into DC line segment and non-DC line segment. To ensure reliable operation of the protection on the DC line, faults in the non-DC line section should be excluded.

From the analysis in Section 3.2.1, it can be seen that when a fault occurs in the DC line, the fault current waveform at the protection installation between the converter stations changes, showing positive correlation, high similarity and small fault distance; when a fault occurs outside the DC line, the fault current waveform at the protection installation of the converter stations changes, showing negative correlation, low similarity and large fault distance;

Extract the minimum distance value of current fault waveform of the DC line between the two-end converter stations, as shown in equation (13).

$$D_1 = \min\left(|D_{\mathrm{allP}}|, |D_{\mathrm{allN}}|\right) \tag{13}$$

According to the difference of current fault waveform distance between internal and external faults, the internal and external faults criterion can be constructed as equation (14)..

$$D_1 < D_{\mathrm{set2}} \tag{14}$$

Where: Dset2 is the setting threshold value. For the selection of Dset2 , it should be able to reliably identify external metallic ground faults and internal high resistance faults. Due to the difference between internal and external faults occurring, a reasonable value of Dset2 is 1.1, based on a large number of simulations and taking into account certain margins. If equation (14) is satisfied, the fault is judged as an internal fault, i.e., the fault occurs on the DC transmission line. Otherwise, it is an external fault, i.e., the fault does not occur on the transmission line.

5.2.3 Fault Pole Identification Criteria: After judging that the fault occurred in the DC line interval, the fault pole was further identified.

Based on the difference between positive and negative pole faults, the fault waveform distances of the two poles are extracted respectively and the ratio of the positive and negative fault waveform distances is further calculated as equation (15).

$$K_2 = \frac{|D_{\mathrm{allP}}|}{|D_{\mathrm{allN}}|} \tag{15}$$

Due to the coupling effect, the fault pole will cause the not-fault pole to induce a certain fault component, and there will be a certain change in the fault current waveform and an increase in the waveform distance for both positive and negative poles. However, due to boundary effects and the relatively small waveform distance of the non-faulted pole, the faulted pole can be reliably determined by selecting a reasonable setting value of K2. The constructed fault pole criterion is shown in (16).

$$\begin{cases} K_2 \leq 0.6 & \text{The positive fault} \\ 0.6 < K_2 \leq 1.5 & \text{Bipolar fault} \\ K_2 > 1.5 & \text{The negative fault} \end{cases} \tag{16}$$

Where: the setting values 1.5 and 0.6 are adjusted according to the reliability and sensitivity requirements.

5.3 Protection process flowchart

Combined with the above fault characteristics analysis and protection criteria, the specific protection process is as follows:

(1) Run the system model, debug the installed protection measuring devices, monitor the electrical quantity signals during normal operation in real time, and observe whether there is abnormal.

(2) Collect the transient electrical quantity signals at the converter stations, and extract the current fault component of the positive and negative DC transmission line. Then the fault can be judged by the protection start criterion. If the criterion is satisfied, it can be known that a fault occurs on the DC line.

(3) Calculate the comprehensive distances of the current fault component waveform of positive and negative poles between the two converter stations, which are denoted as DPX and DNX. Then compare them with the protection setting value Dset1 to determine the fault occurrence interval. When DPX is smaller than the protection setting value Dset1 and DNX is also smaller than the protection setting value Dset1, the fault occurs between the two converter stations, otherwise it occurs between other converter stations.

(4) Compare the minimum value D1 of the comprehensive distance of the positive and negative current fault component waveform between the fault stations with the value of Dset2 to further determine the internal and external faults. When D1 is smaller than the value of Dset2, the current fault component waveform similarity between the two stations is high and the internal fault occurs. When D1 is larger than the value of Dset2, the current fault component waveform similarity between the two stations is low and the external fault occurs.

(5) Calculate the ratio K2 of the comprehensive distance between the positive and negative current waveform, then compare it with the setting value to further identify the fault poles.

When K2 is less than or equal to 0.6, the positive fault occurs;

When K2 is greater than 1.5, the negative fault occurs;

When K2 is larger than 0.6 and less than or equal to 1.5 bipolar fault occurs.

The overall protection process is shown in Fig.5.

Fig.5 Flexible DC Grid Protection Flowchart Based on the Current Fault Component Waveform Similarity

Simulation results verification

Based on the actual parameters of the Zhangbei four-terminal flexible DC transmission system, the PS-CAD/EMTDC simulation platform was used to build a model and debug the relevant electrical parameters to simulate the occurrence of various faults under different operating conditions. The fault is assumed to occur between station B3 and station F1, and the simulation duration is 4.5s. The fault occurs at 3.5s and lasts for 0.1s, the fault sampling frequency is 10kHz and the sampling window length is 0.4ms.

6.1 Distinction between fault lines and non-fault lines

According to the fault characteristic analysis, when a fault occurs between the different converter stations, the current fault component waveform similarity between converter stations will change. If a fault occurs at the point f1 on the DC line between B3 station and F1 station, the positive and negative current fault components of each protection measurement installation point are extracted, and the comprehensive distance between the positive and negative current fault component waveforms of the two stations are calculated as DPX and DNX. The calculation results of the comprehensive distance are listed in Table 3.

Table 3 Waveform distance of positive and negative current fault component when a fault occurs on the DC line at the fault Point f1 between station B3 and station F1

Converter station	Protection Measurement Installation Point	D_{PX}	D_{NX}
B2-E1	1、8	2.1367	2.1722
B2-B3	2、3	2.3962	2.3867
B3-F1	4、5	0.3741	0.6432
E1-F1	6、7	2.3165	2.3323

From Table 3, it can be seen that when a fault occurs between the preset station B3 and F1, the waveform distances of DPX and DNX between the positive and negative current fault component of the converter stations on both sides are less than the setting value Dset1, which is equal to 1, indicating a high waveform similarity. The DPX and DNX values between other stations are higher than those of the preset station B3-F1, and the waveform similarity is low. Therefore, according to (12), it can be determined that the fault occurs between station B3 and station F1. For various fault types, simulation verification between different stations is carried out. The simulation results show that the fault waveform similarity is different when a fault is set between stations. The difference can effectively distinguish fault interval from non-fault interval.

When the fault occurs between the preset stations b3-F1, On the contrary, the VALUES of DPX and DNX between other stations are greater than Dset1, and the waveform similarity is low. Therefore, according to Equation (1.12), it can be determined that the fault occurs between B3 station and F1 station. For different fault types, simulation verifications between different stations are carried out. The simulation results show that the fault waveform similarity is different when the fault settings are located between different stations. The difference can be used to identify the fault interval from the non-fault interval. Due to space limitations, the simulation results are omitted.

6.2 Internal and external fault simulation results

The setting value should take into account the most severe fault situation.

When the current fault waveform similarity is used to identify the internal and external faults, it should be able to distinguish the internal fault with high resistance from the external metallic ground fault.

Similarly, the internal fault locations from f1 to f4 are set between the two protection installation points of the DC line and the external metallic ground fault locations from f5 to f8 are set at the exit of the converter. For different positions, transition resistance and fault type, the fault simulations are carried out as follows.

6.2.1 Metal grounding fault simulation results: By running the system model and conducting fault simulation for each fault type, the simulation results of metallic ground faults of internal and external faults can be obtained, respectively, as shown in Fig.6 and Fig.7.

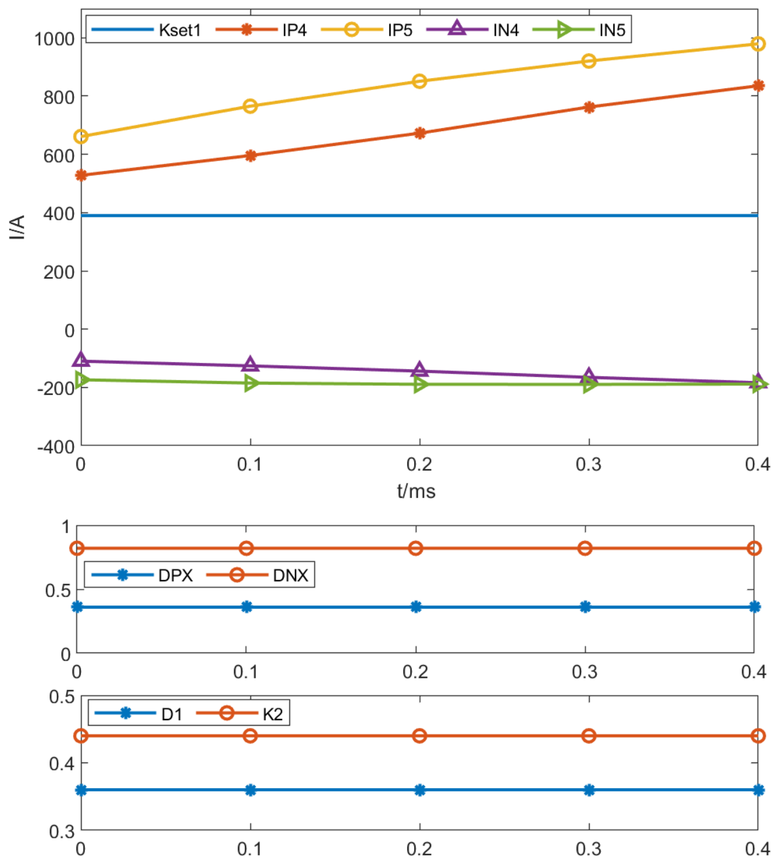

Simulation results at the fault point f1

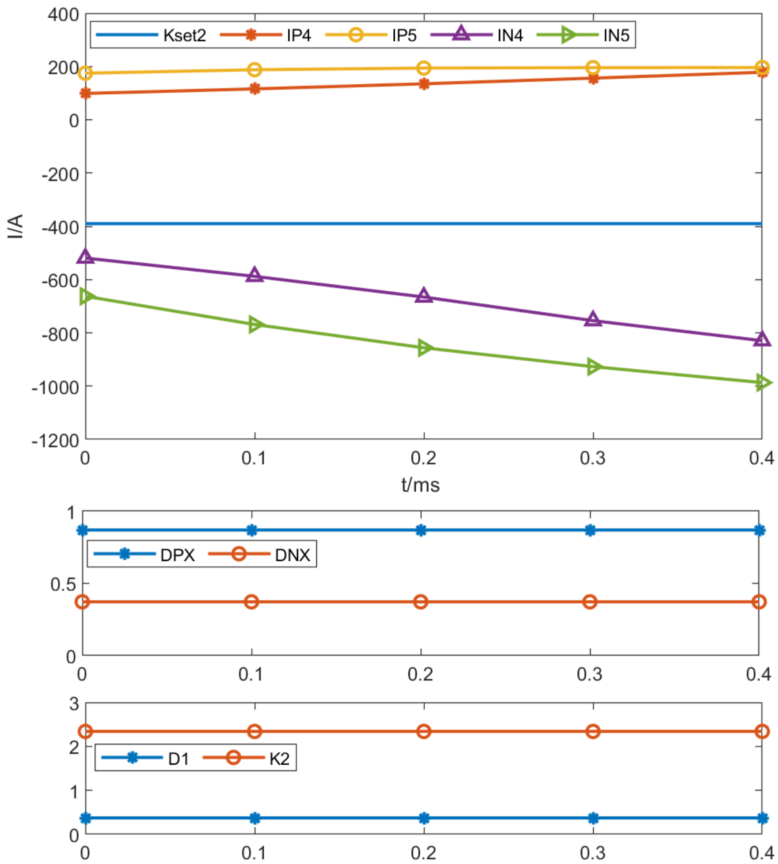

Simulation results at the fault point f2

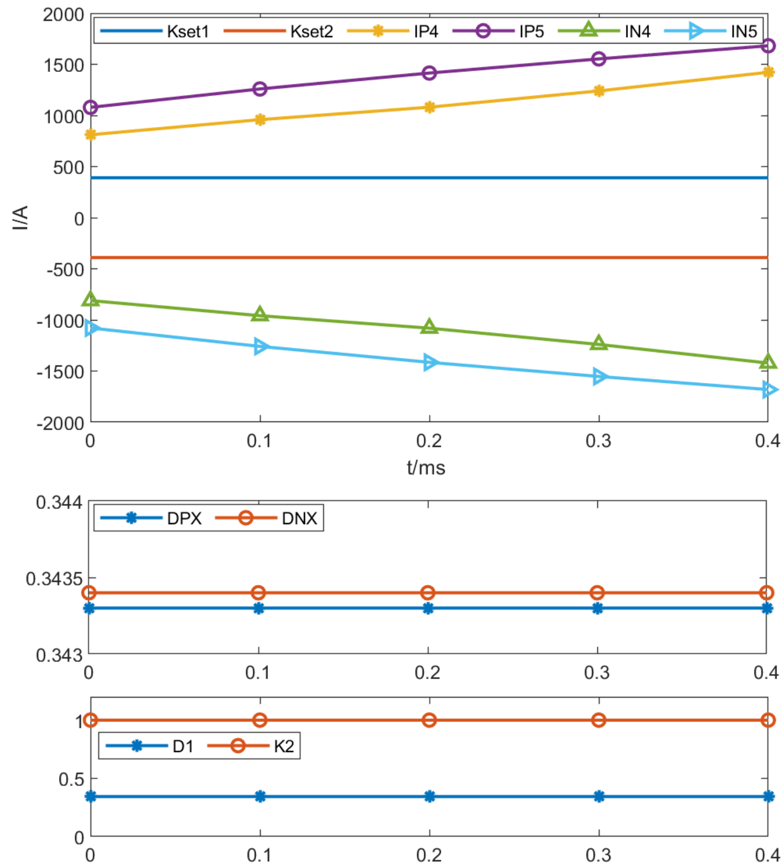

Simulation results at the fault point f3

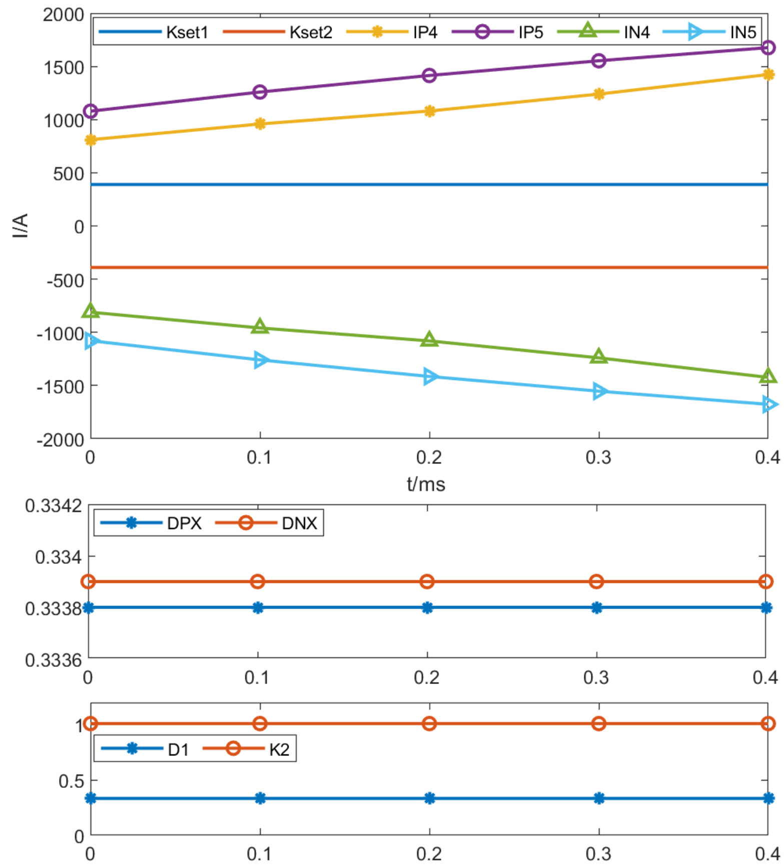

Simulation results at the fault point f4

Fig .6 Simulation of the current fault component waveform when an internal fault occurs

From Fig. 6, it can be seen that when an internal fault occurs on the DC line the fault components of the positive current at 4 and 5 of the converter stations on both sides are both positive, and the fault components of the negative current are both negative. The fault current waveforms collected by the corresponding poles are positively correlated, with high similarity and small waveform distance.

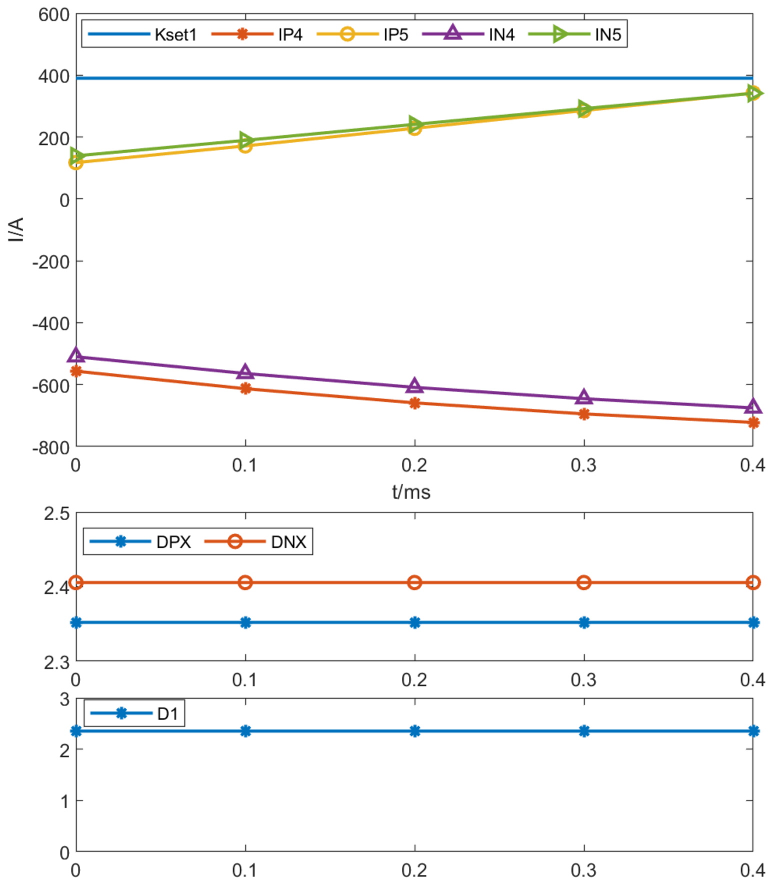

Simulation results at the fault point f5

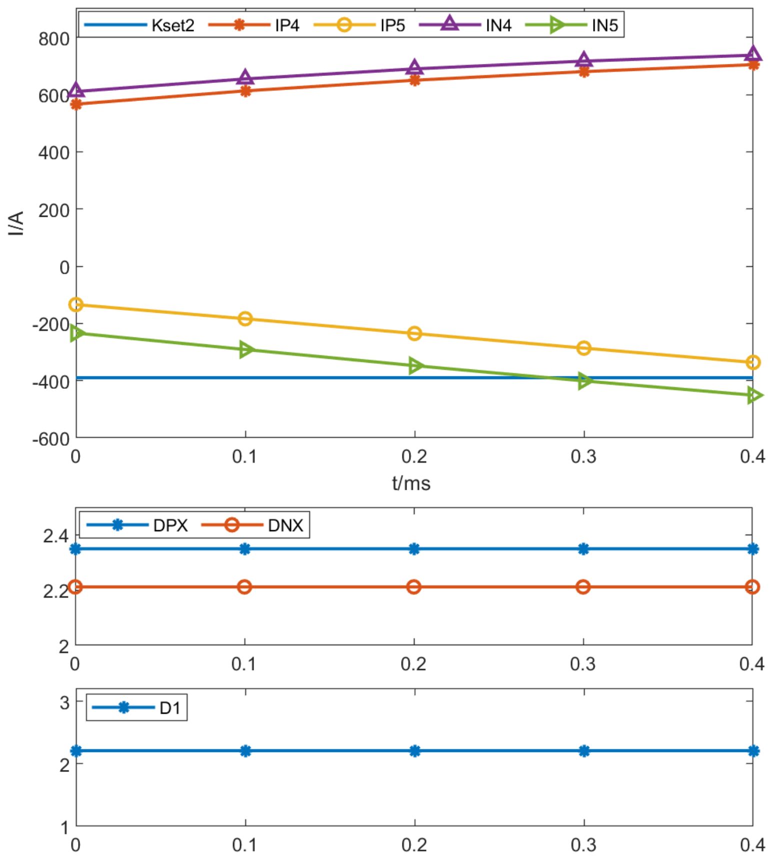

Simulation results at the fault point f6

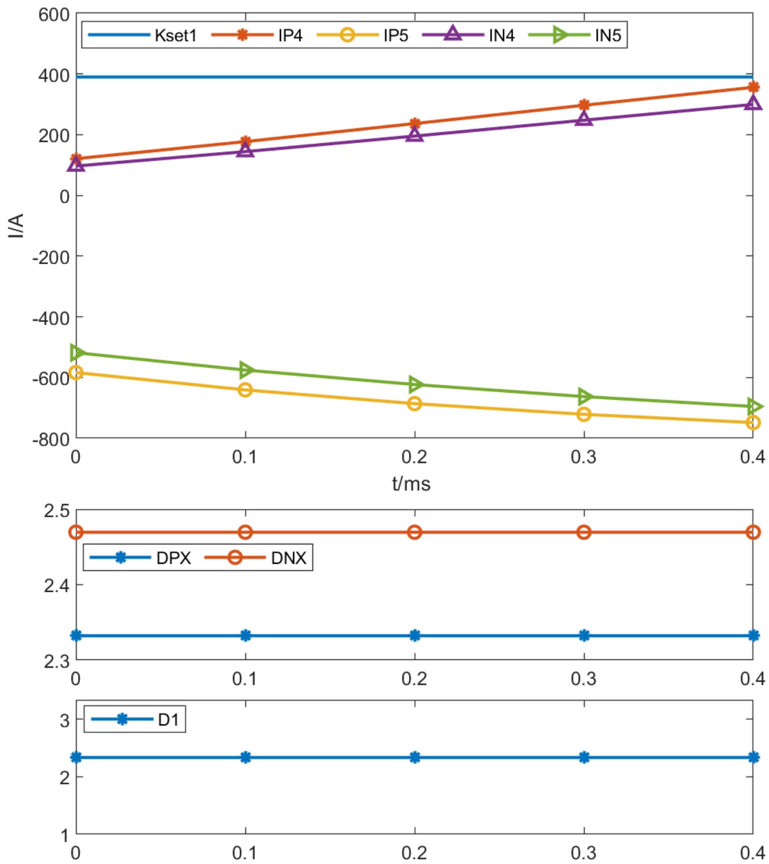

Simulation results at the fault point f7

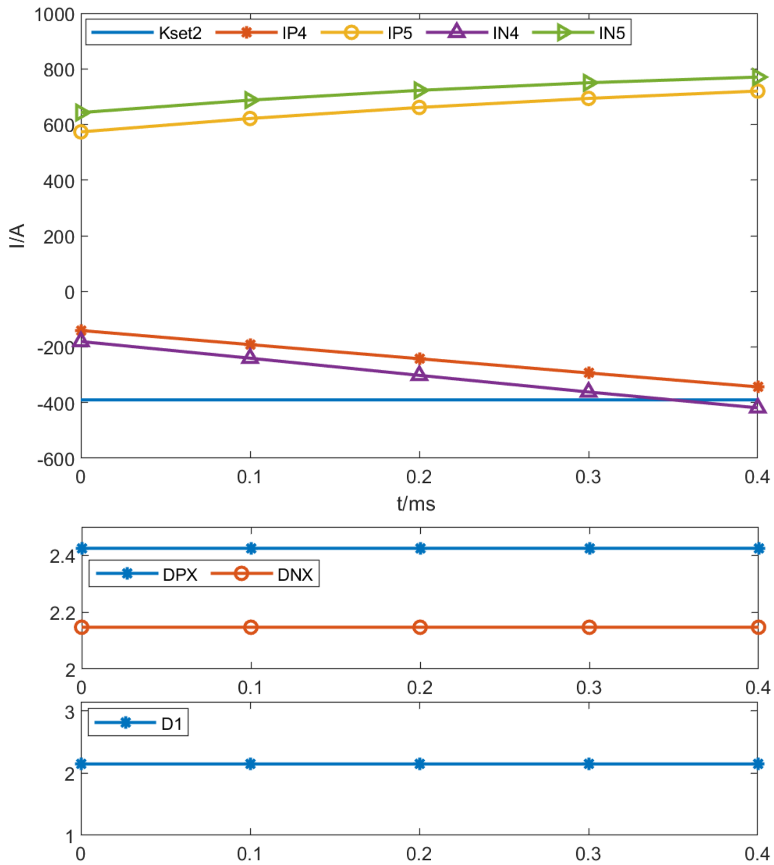

Simulation results at the fault point f8

Fig.7 Simulation of the current fault component waveform when an external fault occurs

From Fig.7, it can be seen that: when a fault occurs beyond the DC line, the fault components of positive and negative current at 4 and 5 stations on both sides are positive or negative, and the current fault component waveforms collected by the corresponding poles are negatively correlated, with low similarity and large waveform distance.

In order to explore the sensitivity of line end protection, simulation verifications are carried out for different fault locations and fault types, and the comprehensive distance DallP and DallN of current fault waveform are calculated, and D1 value could be obtained after comparison. Simulation verification results is shown in Table 4.

Table 4 Identification results of metal short circuit of internal and external fault

Fault type	Fault position			D_1	Identifi
f_1	10% distance of the total line from rectifier side protection installation	**0.3601**	**0.8236**	**0.3601**	Interna
	90% distance of the total line from rectifier side protection installation	**0.3891**	**0.8193**	**0.3891**	
f_2	10% distance of the total line from rectifier side protection installation	**0.8693**	**0.3722**	**0.3722**	Interna

Fault type	Fault position			D_1	Identifi
	90% distance of the total line from rectifier side protection installation	**0.8744**	**0.2887**	**0.2887**	
f_3	10% distance of the total line from rectifier side protection installation	**0.3433**	**0.3434**	**0.3433**	Interna
	90% distance of the total line from rectifier side protection installation	**0.6790**	**0.6790**	**0.6790**	
f_4	10% distance of the total line from rectifier side protection installation	**0.3338**	**0.3338**	**0.3338**	Interna
	90% distance of the total line from rectifier side protection installation	**0.2110**	**0.2110**	**0.2110**	
f_5	Rectifier side converter outlet	**2.3521**	**2.4055**	**2.3521**	Externa
f_6	Rectifier side converter outlet	**2.3496**	**2.2115**	**2.2115**	Externa
f_7	inverter side converter outlet	**2.3323**	**2.4696**	**2.3323**	Externa
f_8	inverter side converter outlet	**2.4247**	**2.1470**	**2.1470**	Externa

Combined with the fault identification criteria (13) and (14), Table 4 shows that: when a fault occurs on the positions f1, f2 , f3 and f4 , the values of D1 of them are less than the setting value of Dset2, which is equals to 1.1, indicating that the fault is an internal fault; when a fault occurs on the positions f5, f6 , f7 and f8, the values of D1 of them are greater than the setting value of Dset2, which is equals to 1.1, indicating that the fault is an external fault. To sum up, when the metallic short circuit fault occurs, the proposed protection criterion can reliably distinguish whether a fault occurs on or beyond the DC line.

6.2.2 High transition resistance simulation results : When a short-circuit fault occurs on a DC line, the transition resistance value can affect the reliability and sensitivity of the protection.

Due to its limiting effect, the comprehensive distance of current fault waveform fluctuates to a certain extent, so it is necessary to conduct simulation verification for different transition resistances.

Take fault f1 as an example, set the transition resistance as 500 Ω, and keep the other parameters unchanged. Fig.8 shows the simulation results.

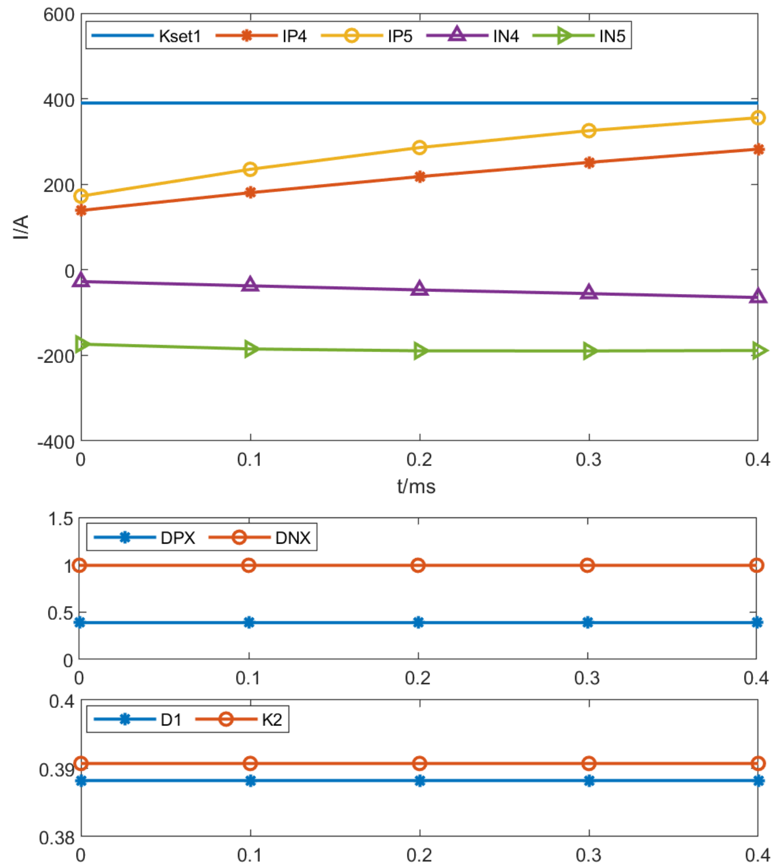

Φιγ .8 Σιμυλατιον ρεσυλτς ωιτη τηε τρανσιτιον ρεσιστανςε οφ 500Ω ατ τηε φαυλτ ποιντ φ1

As can be seen from Fig.8, when a fault with the transition resistance 500Ω occurs on the point f1, the fault components of the positive current at 4 and 5 of the converter stations on both sides are both positive, and the fault components of the negative current are both negative. The current fault component waveforms collected from the corresponding poles are positively correlated, with high similarity and small waveform distance. Further, the corresponding current fault waveform distance D1 is equal to 0.3882, which is smaller than the setting value of Dset2. According to the protection criterion, the fault is judged to be an internal fault.

In order to explore whether the protection works reliably and quickly when other high resistance faults occur, simulations were carried out for 250Ω and 500Ω transition resistors in different fault location respectively. And the simulation results are shown in Table 5.

Table 5 Fault identification results of high transition resistance of internal and external fault

Fault type	Fault location	Transition resistance/Ω	D_{allP}	D_{all}
f_1	10% distance of the total line from rectifier side protection installation	250	0.3732	0.91
		500	0.3882	0.99

Fault type	Fault location	Transition resistance/Ω	D_{allP}	D_{all}
	90% distance of the total line from rectifier side protection installation	250	0.3729	0.92
		500	0.3661	1.04
f_2	10% distance of the total line from rectifier side protection installation	250	0.9265	0.38
		500	0.9899	0.43
	90% distance of the total line from rectifier side protection installation	250	0.9219	0.34
		500	0.9974	0.37
f_3	10% distance of the total line from rectifier side protection installation	250	0.4137	0.41
		500	0.4493	0.44
	90% distance of the total line from rectifier side protection installation	250	0.3825	0.38
		500	0.4165	0.41
f_4	10% distance of the total line from rectifier side protection installation	250	0.4064	0.40
		500	0.4500	0.45
	90% distance of the total line from rectifier side protection installation	250	0.3723	0.37
		500	0.4070	0.40

As can be seen from Table 5, when high-resistance faults occur on DC lines, the values of D1 at the fault points f1, f2, f3 and f4 are all less than smaller than the setting value of Dset2.

Therefore, according to the protection criterion, the faults are judged to be internal faults.

Combined with Table 4 and 5, the proposed protection criteria can accurately identify internal and external faults. In the case of a high transition resistance at the end of the line, when the fault occurs in the DC line, the protection can also operate reliably and remove the high resistance fault quickly. When the fault occurs outside the DC line, the protection will operate correctly.

In order to explain more clearly the question, combining Tables 4 and 5 above, the results of the internal and external fault identification can be obtained, as shown in Fig.9. In Fig.9, f1 (10%) represents the simulation result of a fault f1 occurring 10% distance of the total line from rectifier side, similar for other fault types.

Hosted file

`image23.emf` available at https://authorea.com/users/617453/articles/642877-new-pilot-protection-method-based-on-the-current-fault-component-waveform-similarity

Fig.9 Simulation results for internal and external faults identification

As can be seen from Fig.9, the proposed protection criteria can accurately identify internal and external faults. When a fault with high transition resistance (500 Ω) occurs at the end of the line, the protection can also act reliably and quickly remove the fault. And when a fault occurs outside the DC line, the protection will operate correctly.

6.3 Fault pole identification simulation results

After determining the internal and external faults, fault pole identification should be carried out for the fault occurring at the points of f1, f2, f3 and f4. f1 and f2 simulate single pole earth faults, which are positive and negative earth faults respectively; f3 and f4 simulate double pole faults, which are double pole crossover faults and double pole short circuit earth faults respectively. The ratio K2 of the positive and negative current fault waveform distances is calculated and the resulting values of K2 are shown in Table 6.

Table 6 The value of K2 of fault pole identification with different transition resistance

Fault Type	Fault grounding resistance/Ω	The value of
f_1	0.01	0.44

Fault Type	Fault grounding resistance/Ω	The value of
	250	0.41
	500	0.39
f_2	0.01	2.34
	250	2.42
	500	2.27
f_3	0.01	1.00
	250	0.99
	500	0.99
f_4	0.01	1.00
	250	1.01
	500	0.98

As can be seen from Table 6, when a positive earth fault (f1) occurs on the DC line, the respective K2 values are less than 0.6 for each earth resistance case; when a negative earth fault (f2) occurs on the DC line, the respective K2 values are greater than 1.5 for each earth resistance case; when a double pole crossover fault (f3) and a double pole crossover earth fault (f4) occur, the respective K2 values are greater than 0.6 and less than 1.5, which are in accordance with the fault pole identification criterion. Therefore, according to the fault pole identification criteria, the identification of the fault poles can be achieved.

6.4 Protection action results

Combining the analysis in Section 3.1 with the simulation results in Section 6.1-6.3, the final protection actions are shown in Table 7.

Table 7 Protection action results during fault simulation

Type of fault	Wave correlation	Identification results	Protection operation
f_1	Positive correlation, high similarity	Internal fault	P_4、P_5 operation
f_2	Positive correlation, high similarity	Internal fault	N_4、N_5 operation
f_3	Positive correlation, high similarity	Internal fault	P_4、P_5、N_4 and N_5 operation
f_4	Positive correlation, high similarity	Internal fault	P_4、P_5、N_4 and N_5 operation
f_5	Negative correlation, low similarity	External fault	No operation
f_6	Negative correlation, low similarity	External fault	No operation
f_7	Negative correlation, low similarity	External fault	No operation
f_8	Negative correlation, low similarity	External fault	No operation

Table 7 shows that in the event of a single pole fault occurring on the DC line, the corresponding fault pole protection will operate and remove the fault, while the sound pole protection will operate correctly and it can still operate; in the event of a double pole fault occurring on the DC line, both pole protections will operate; in the event of a fault occurring outside the DC line, the protection will operate correctly.

When a fault occurs, the current fault component changes quickly, and the protection can be started at about 0.5ms. Current fault waveform collection and comprehensive distance calculation can be completed in 1ms. With a certain margin, the protection scheme proposed in this paper can operate reliably within 2ms, and the reliability and rapidity are further improved with a high transition resistance.

Conclusions

This paper analyzes the current fault characteristics of multi-terminal flexible DC power grid, introduces the comprehensive distance of current fault waveform, and proposes a line protection scheme based on the similarity of current fault waveform. By combining Euclidean DTW distance and entropy weight method to deal with current fault component waveform signal, the comprehensive distance of current fault component waveform of the DC line is calculated, and the similarity protection criterion is constructed. The calculated comprehensive distance is used to realize internal and external faults identification, and the ratio of positive and negative comprehensive distance and pole comprehensive distance is used to realize fault pole identification. PSCAD is used to build a flexible DC grid model to simulate different fault conditions and transition resistances, so as to output fault data under different fault conditions. MATLAB is used to analyze and process fault data to verify the protection algorithm. A large number of simulation results show that when a fault occurs, the fault pole protection does not refuse to operate, the non-fault pole protection does operate correctly, and the protection action time is very short. Therefore, the protection scheme proposed has high reliability, its rapidity and adaptability are further improved. And it has a certain ability to resist transition resistance. The research results will provide a theoretical basis for the safe and reliable operation of flexible DC power grid.

Acknowledgments

This work is supported by the National Natural Science Foundation of China (No. 51777166), Key support projects of the National Natural Science Foundation (No. U1766209).

References

1. Leon AE: 'Short-Term Frequency Regulation and Inertia Emulation Using an MMC-Based MTDC System,' IEEE Transactions on Power Systems,2018, 33, (3), pp2854-2863.
2. S. Debnath, J. Qin, B. Bahrani, M. Saeedifard, and P. Barbosa: ' Operation, control, and applications of the modular multi-level converter: a review,' IEEE Transactions on Power Electronics,2015,30, (1), pp37-53.
3. J. Zheng, M. Wen, Y. Qin, et al.: 'A novel pilot directional backup protection scheme based on transient currents for HVDC lines,' International Journal of Electrical Power and Energy Systems, 2020,115, pp1-9.
4. X. Han, W. Sima, M. Yang, L. Li, T. Yuan, and Y. Si: 'Transient characteristics underground and short-circuit faults in a ±500 kV MMC-based HVDC system with hybrid DC circuit breakers', IEEE Transactions on Power Delivery, 2018, 33(3), pp1378-1387.
5. Q. Huang, G. Zou, S. Zhang, et al.: 'A Pilot Protection Scheme of DC Lines for Multi-Terminal HVDC Grid,' IEEE Transactions on Power Delivery,2019,34, (5), pp1957-1966.
6. X. Dong, L. Tang, S. Shi, Y. Qiu, M. Kong, and H. Pang: 'Configuration Scheme of Transmission Line Protection for Flexible HVDC Grid,' Power Syst Technol., 2018, 42, (6), pp1752–1759.
7. Sneath J., Rajapakse AD.: 'Fault Detection and Interruption in an Earthed HVDC Grid Using ROCOV and Hybrid DC Breakers,' IEEE Transactions on Power Delivery,2016, 31, (3), pp 973-981.
8. Leterme W., Beerten J., Van Hertem D.: 'Nonunit Protection of HVDC Grids with Inductive DC Cable Termination,' IEEE Transactions on Power Delivery, 2016, 31, (2), pp 820-828. Z. X. Zhou, H. Cao, H. Z. Liu, X. G Wang, & D. X. Du. Dual-terminal current accumulation protection of HVDC transmission lines considering the influence of inter-pole mutual inductance. Chinese Journal of Electrical Engineering ,1-13.
9. Li R., Xu L., Yao L.: 'DC Fault Detection and Location in Meshed Multiterminal HVDC Systems

Based on DC Reactor Voltage Change Rate,' IEEE Transactions on Power Delivery, 2017, 32, (3), pp1516-1526.

10. Li B., Li Y, He J, Wen, W.: 'A Novel Single-Ended Transient-Voltage-Based Protection Strategy for Flexible DC Grid ',IEEE Transactions on Power Delivery, 2019, 34, (5), pp1925-1937.
11. Xiang W., Yang S., Xu L., J., etal.: ' A transient voltage-based DC fault line protection scheme for MMC-based DC grid embedding DC breakers,' IEEE Transactions on Power Delivery, 2019, 34, (1), pp334-345.
12. Kong F., Hao Z., Zhang B.: 'A Novel Traveling-Wave-Based Main Protection Scheme for +-800 kV UHVDC Bipolar Transmission Lines', IEEE Transactions on Power Delivery, 2016,31, (5), pp 2159-2168.
13. Li Y., Wu L., Li J., Xiong L., et al.: 'DC Fault Detection in MTDC Systems Based on Transient High Frequency of Current,' IEEE Transactions on Power Delivery, 2019,34, (3), pp950-962.
14. Jiang L., Chen Q., Huang W., et al.: ' A novel directional pilot protection method for VSC-MTDC based on the initial forward and backward travelling wave head', International Journal of Electrical Power and Energy Systems, 2019, 109, pp198-206.
15. Huang Q., Zou G., Zhang S., Gao H.: 'A Pilot Protection Scheme of DC Lines for Multi-Terminal HVDC Grid', IEEE Transactions on Power Delivery, 2019, 34, (5), pp1957-1966.
16. Li C., Gole A.M., Zhao C.: ' A Fast DC Fault Detection Method Using DC Reactor Voltages in HVDC Grids', IEEE Transactions on Power Delivery, 2018, 33, (5), pp2254-2264.
17. Liu J., Tai N., Fan C.: 'Transient-Voltage-Based Protection Scheme for DC Line Faults in the Multi-terminal VSC-HVDC System', IEEE Transactions on Power Delivery, 2017, 32, (3), pp1483-1494.
18. Liu J., Tang N., Fan C., Yang Y.:'Transient measured impedance-based protection scheme for DC line faults in ultra high-voltage direct-current system', IET Generation Transmission and Distribution, 2016,10, (4), pp 3597-3609.
19. Yang Y., Tai N., Fan C., etal: 'Resonance frequency-based protection scheme for ultra-high-voltage direct-current transmission lines', IET Generation Transmission and Distribution,2018,12, (2), pp318-327.
20. Wang, Y., Yuan, Z., Wen, W., etal: 'Generalised protection strategy for HB-MMC-MTDC systems with RL-FCL under DC faults', IET Generation Transmission and Distribution,2018,12, (2), pp1231-1239.
21. Gupta O., Tripathy M.: 'Universal pilot relaying scheme for series and shunt-compensated lines', IET Generation Transmission and Distribution,2018,12, (4), pp799-806.
22. Tong N., Lin X., Li Y., Hu Z., etal: 'Local Measurement-Based Ultra-High-Speed Main Protection for Long Distance VSC-MTDC', IEEE Transactions on Power Delivery, 2019, 34, (1), pp353-364.
23. Liu X., Osman A.H., Malik O.P: 'Hybrid Traveling Wave/Boundary Protection for Monopolar HVDC Line', IEEE Transactions on Power Delivery,2009,24, (2), pp569-578.
24. Wang Congbo, Jia Ke, Bi Tianshu, Zhao Qijuan, Zhu Rui. Flexible DC distribution line protection based on the similarity identification of transient current waveform [J]. Power Grid Technology, 2019,43(10):3823-3832.
25. Li Zhao, Zheng Yuchao. Failure-adaptive reclosing scheme of multi-terminal flexible straight power grid based on waveform similarity characteristics [J/ OL]. High-voltage technology:1-14[2022-05-10].
26. Zhang Dahai, Wu Chuanjian, and Jinghan, Liang Chenguang, & Li Meng. Flexible DC transmission line backup protection scheme for measuring wave impedance to Euclidean distance. Grid Technology, 1-12.
27. Song Junying, Cui Yiwei, Li Xinran, et al. Load Curve Clustering Method Based on Euclidean Dynamic Time Bending Distance and Enropy Weight Method [J]. Power System Automation, 2020,44 (15): 87-94